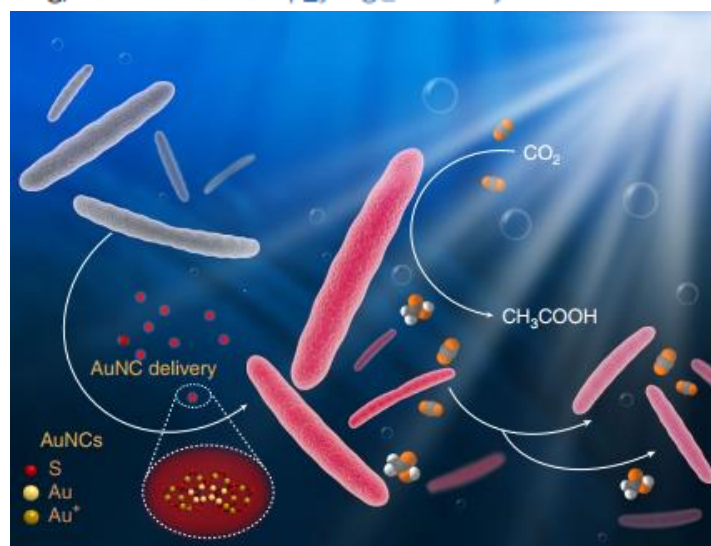


# Bacteria photosensitized by intracellular gold nanoclusters for solar fuel production

Hao Zhang<sup>1,7</sup>, Hao Liu<sup>1,7</sup>, Zhiquan Tian<sup>1,2</sup>, Dylan Lu<sup>1,3</sup>, Yi Yu<sup>1,4</sup>, Stefano Cestellos-Blanco<sup>5</sup>,  
Kelsey K. Sakimoto<sup>1</sup> and Peidong Yang<sup>1,3,5,6\*</sup>

<sup>1</sup>Department of Chemistry, University of California, Berkeley, Berkeley, CA, USA. <sup>2</sup>Key Laboratory of Analytical Chemistry for Biology and Medicine (Ministry of Education), College of Chemistry and Molecular Sciences, Wuhan University, Wuhan, P. R. China. <sup>3</sup>Chemistry Sciences Division, Lawrence Berkeley National Laboratory, Berkeley, CA, USA. <sup>4</sup>School of Physical Science and Technology, ShanghaiTech University, Shanghai, China. <sup>5</sup>Department of Materials Science and Engineering, University of California, Berkeley, Berkeley, CA, USA. <sup>6</sup>Kavli Energy NanoSciences Institute, Berkeley, CA, USA. <sup>7</sup>These authors contributed equally: Hao Zhang, Hao Liu. \*e-mail: [p\\_yang@berkeley.edu](mailto:p_yang@berkeley.edu)



Jenifer  
16.11.19

# Relevance

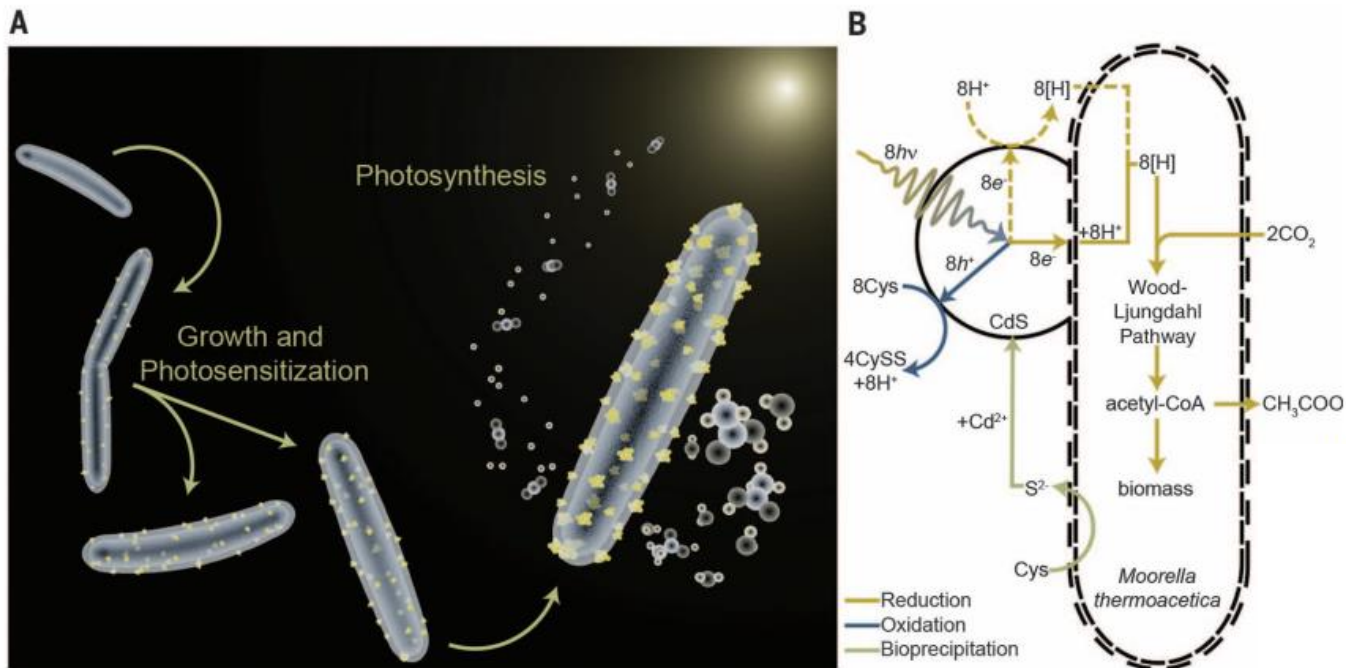
- CO<sub>2</sub> fixation
- Application of clusters in biology, energy and environment.

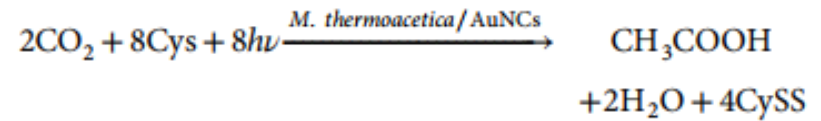
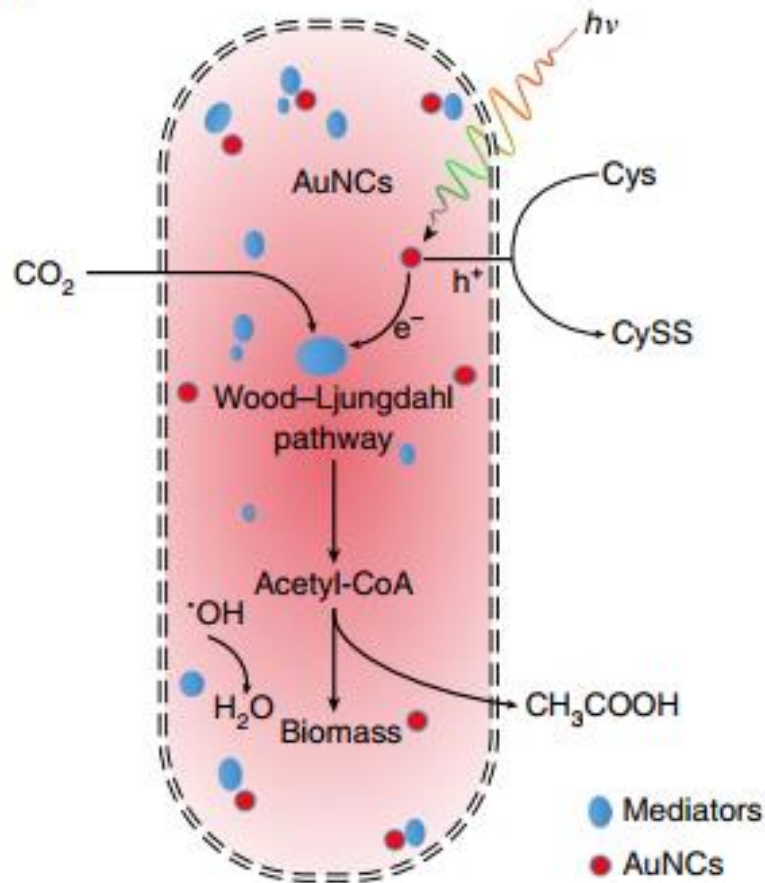
# Significance

- Solar-driven conversion of carbon dioxide to value-added carbon products is an ambitious objective of ongoing research efforts.
- However, high overpotential, low selectivity and poor CO<sub>2</sub> mass transfer plague purely inorganic electrocatalysts.
- Combining the streamlined CO<sub>2</sub> fixation pathways of bacteria with the exceptional ability of nanomaterials to harvest solar energy.

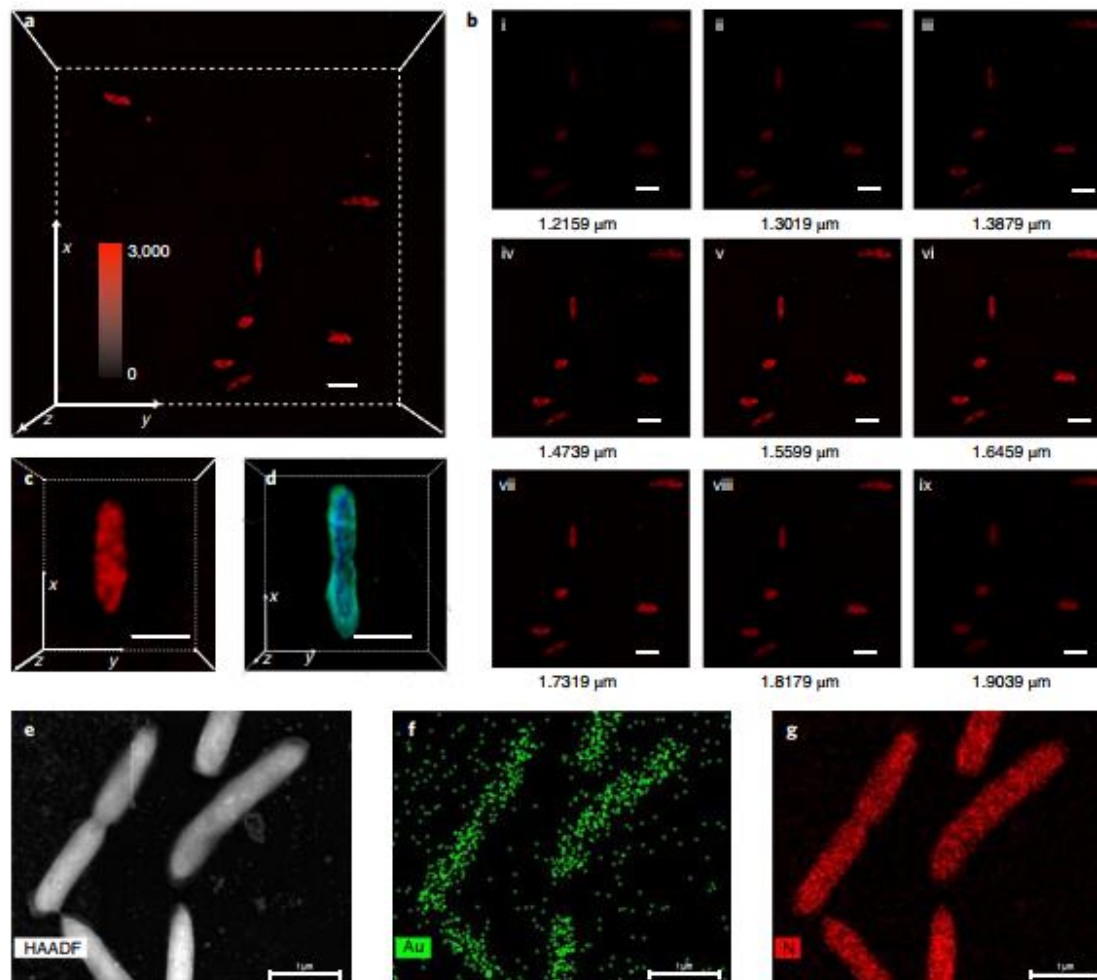
# Self-photosensitization of nonphotosynthetic bacteria for solar-to-chemical production

Kelsey K. Sakimoto,<sup>1,2</sup> Andrew Barnabas Wong,<sup>1,2</sup> Peidong Yang<sup>1,2,3,4\*</sup>

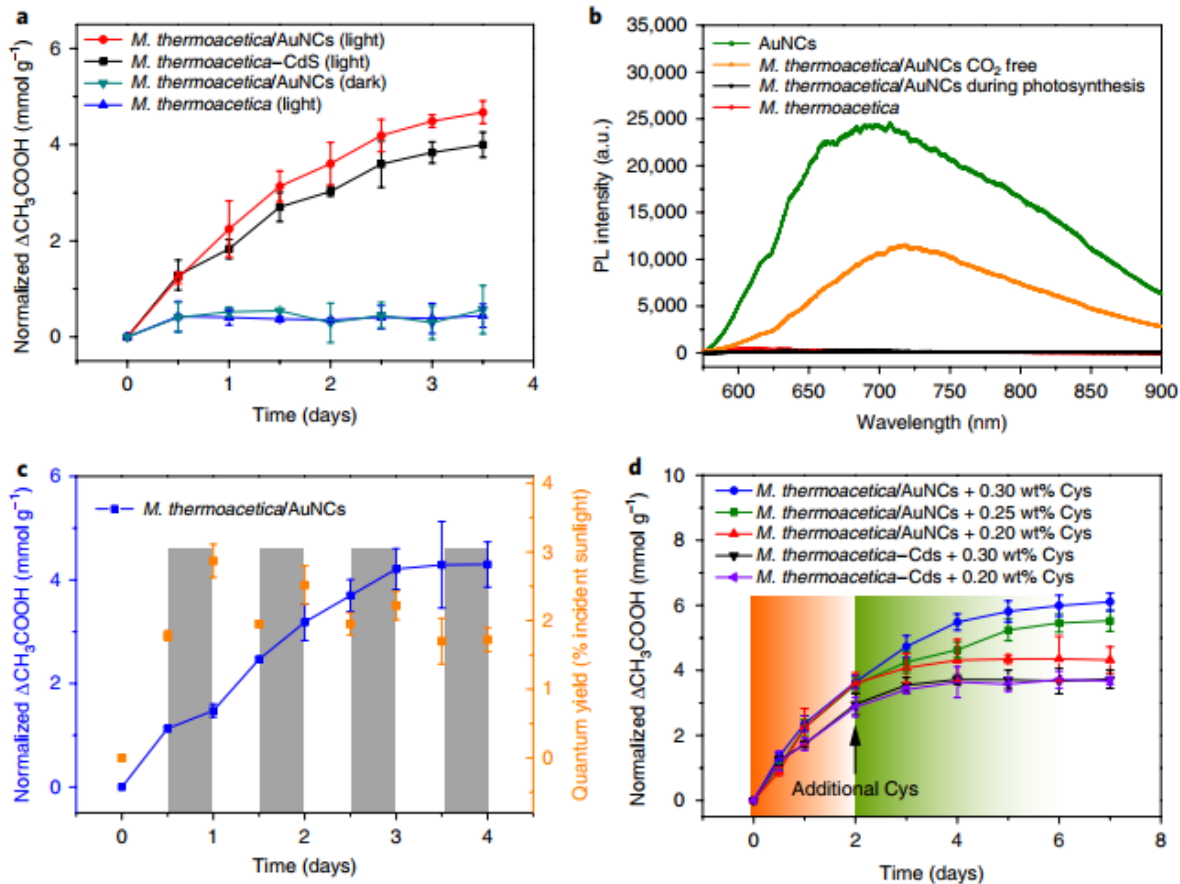


**b**

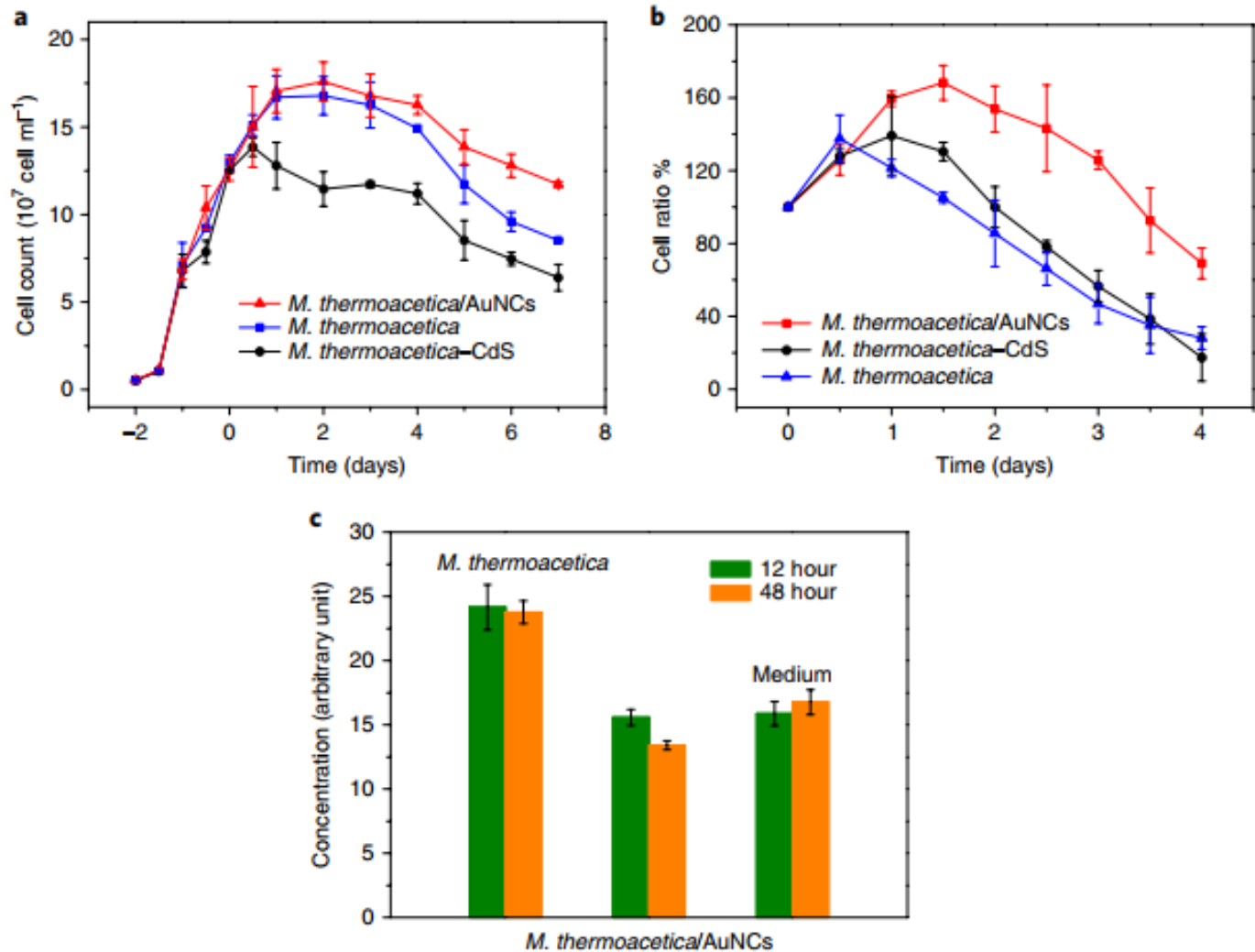
The electrons generated from intracellular AuNCs under illumination are used by enzymatic mediators inside the cytoplasm and are finally passed on to the Wood Ljungdahl pathway.



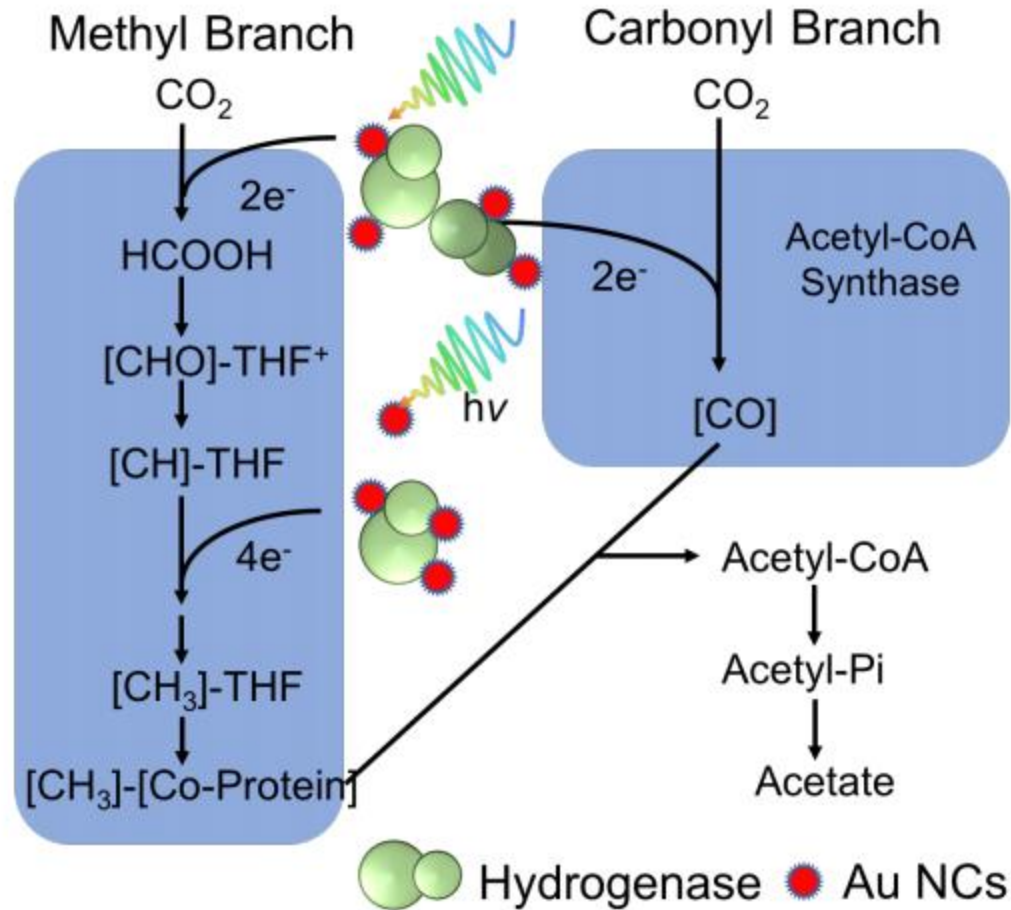
Microscopy images of the *M. thermoacetica*/AuNC hybrid system. **a**, SIM image of several *M. thermoacetica*/AuNCs fluorescing in red (excitation at 540 nm) with total counts ranging from 0 to 3,000. **b**, SIM images of different focal planes (numbered successively i to ix) along the z direction. **c**, SIM image of individual *M. thermoacetica*/AuNC PBS. **d**, SIM image of a single *M. thermoacetica*-CdS PBS (excitation at 408 nm) with annular-shaped emission. **e**, HAADF-STEM image of *M. thermoacetica*/AuNCs. **f**, **g**, EDS mapping of the region in **e**, showing the elements (**f**) Au and (**g**) N across the entire cell. Scale bars for **a-d**, 2  $\mu\text{m}$ .



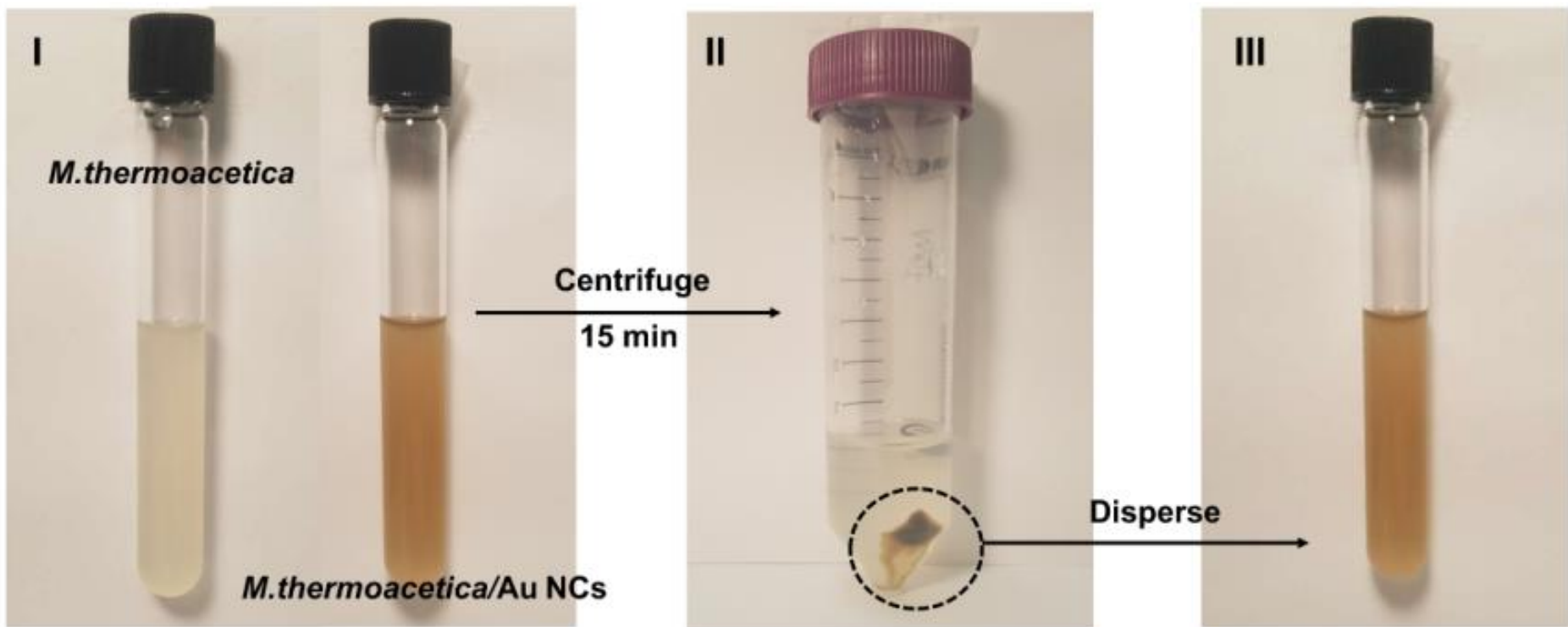
Photosynthesis behaviour of different systems. **a**, Normalized photosynthetic production of acetic acid by *M. thermoacetica*, *M. thermoacetica*/AuNCs and *M. thermoacetica*-CdS PBs under continuous low-intensity illumination and in dark conditions ( $n = 20$  culture batches for *M. thermoacetica*-CdS (light),  $n = 35$  culture batches for other conditions). **b**, Photoluminescence (PL) spectra of pure AuNCs, bare *M. thermoacetica*, *M. thermoacetica*/AuNCs in CO<sub>2</sub>-free conditions without photosynthesis ability, and *M. thermoacetica*/AuNCs in the photosynthesis process. **c**, Normalized acetic acid production and quantum yield of *M. thermoacetica*/AuNCs as percentage of incident light, during light-dark cycles ( $n = 21$  culture batches). **d**, Cysteine dependent acetic acid yield in *M. thermoacetica*/AuNCs and *M. thermoacetica*-CdS with cysteine added at day 2, for 7 days of photosynthesis ( $n = 12$  culture batches). All points and error bars show the mean and standard deviation, respectively, of the experiments.



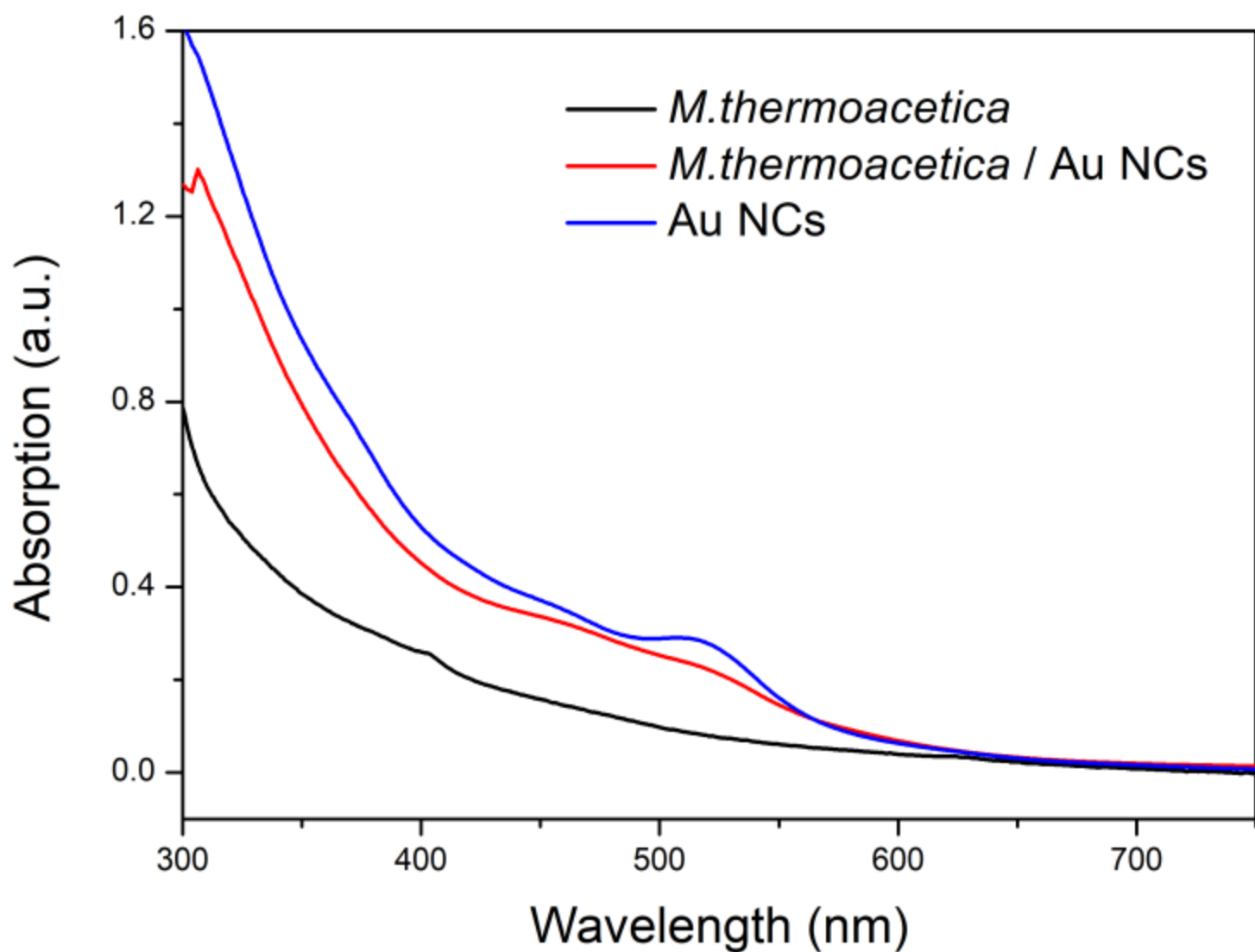
Viability measurements. **a**, **b**, Bacteria enumeration of *M. thermoacetica*/AuNCs, *M. thermoacetica*-CdS and bare *M. thermoacetica* by colony counting in the heterotrophic medium (**a**) in dark conditions and (**b**) in the autotrophic medium exposed to low-intensity illumination ( $n = 20$  culture batches for each condition). **c**, ROS concentration of bare *M. thermoacetica*, *M. thermoacetica*/AuNCs and medium, under low-intensity illumination for 12 h and 48 h ( $n = 9$ ). All points and error bars show the mean and standard deviation, respectively, of the experiments.



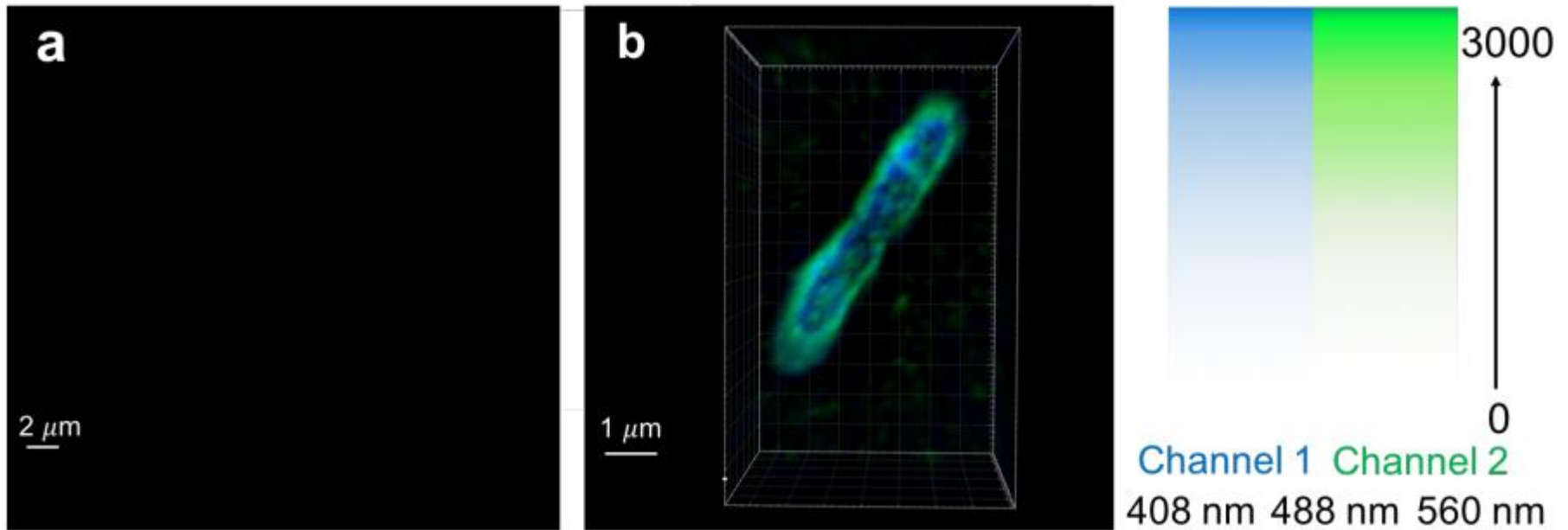
The acetyl-CoA pathway as resolved from *M. thermoacetica*.  
 Abbreviations: THF, tetrahydrofolate; Pi, inorganic phosphate;  
 [e<sup>-</sup>], reducing equivalent; Co-Protein, corrinoid enzyme.



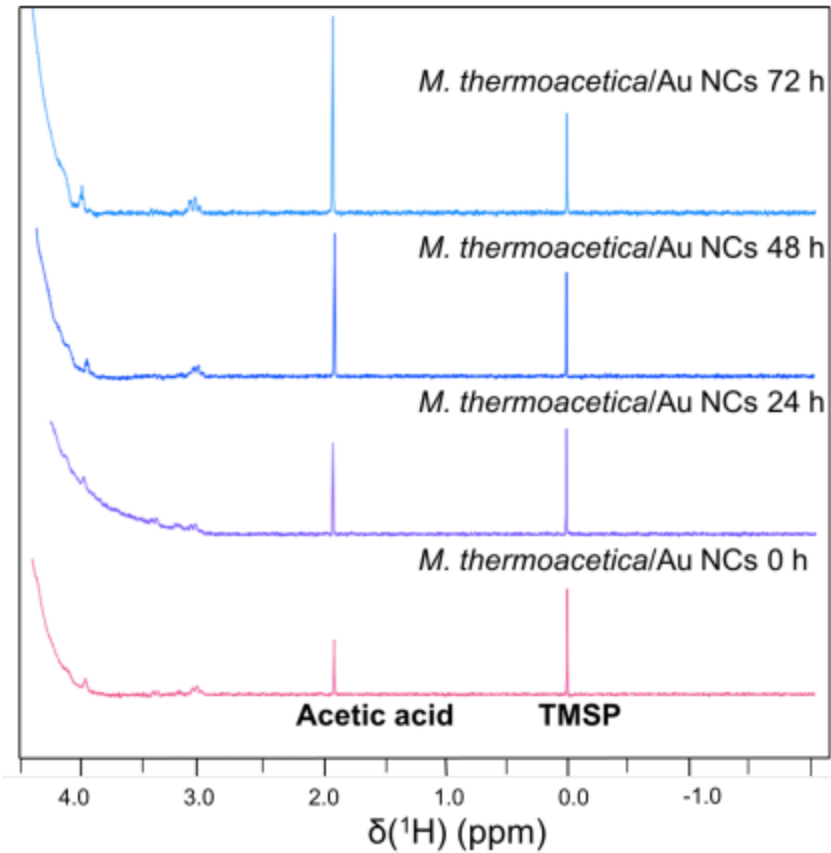
The characterization of *M. thermoacetica*/Au NCs hybrid system and deletional controls. I, picture of the bare *M. thermoacetica* and *M. thermoacetica*/Au NCs with different colors. II, picture displaying the colorless supernatant of *M. thermoacetica*/Au NCs hybrid system after centrifugation. III, picture of redispersed solution from II sediment.



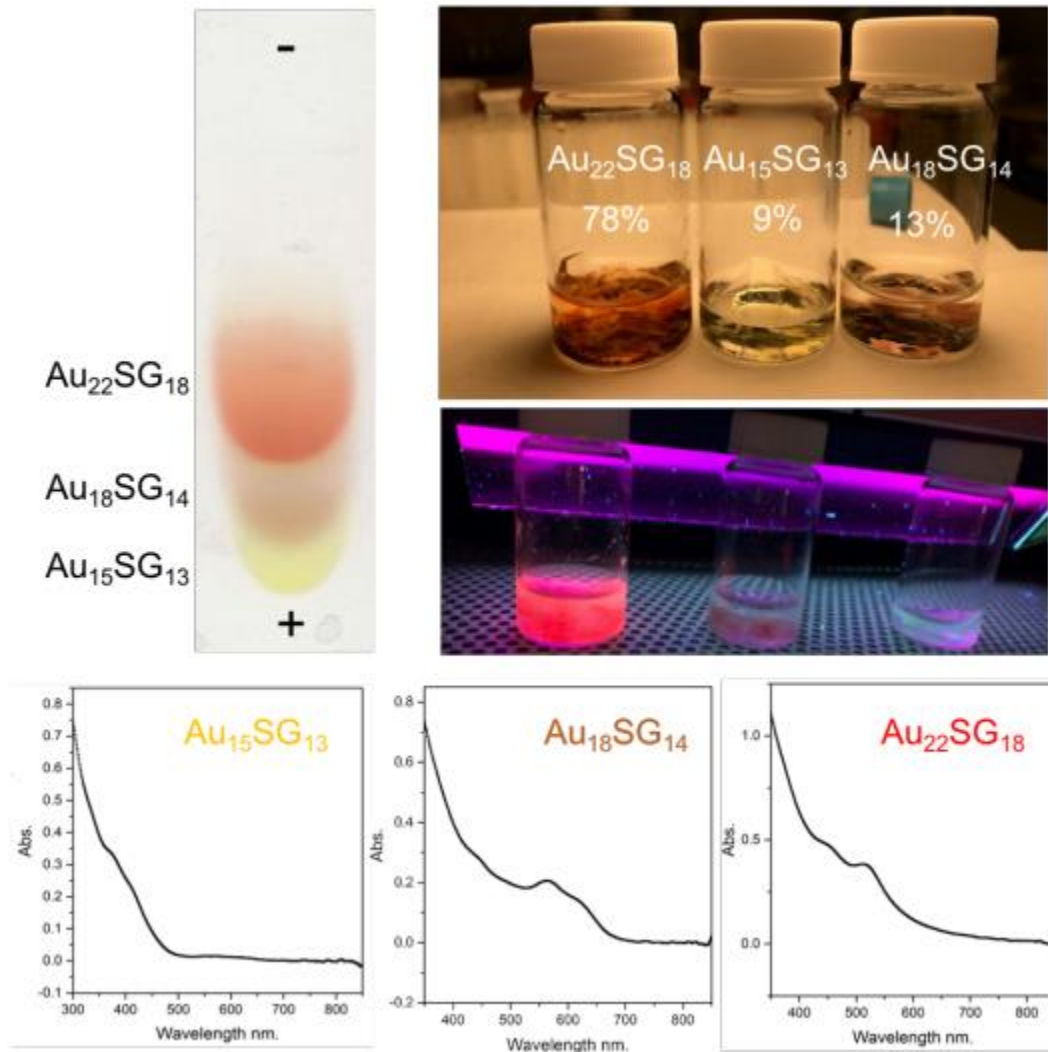
**The characterization of *M. thermoacetica*/Au NCs hybrid system** UV-Vis of bare Au NCs, *M. thermoacetica*, and *M. thermoacetica*/Au NCs. The incident light source could be scattered by large population of bacteria, and the photons that can reach the intracellular Au NCs are much less than that of the bare Au NCs solution. Due to reduced incident light intensity, the intracellular Au NCs shows the same absorption pattern with weaker absorbance value than the bare Au NCs solution.



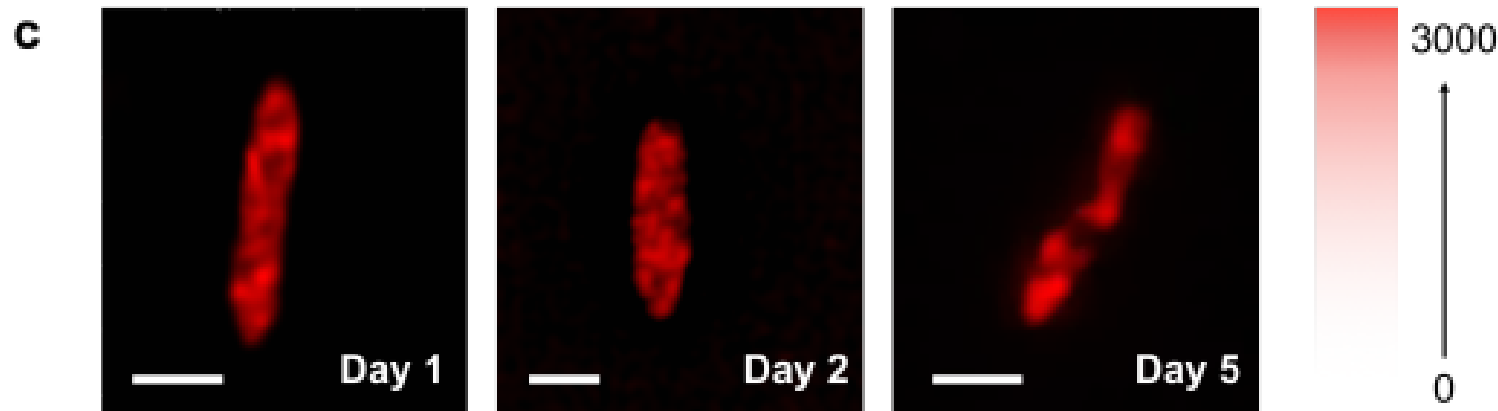
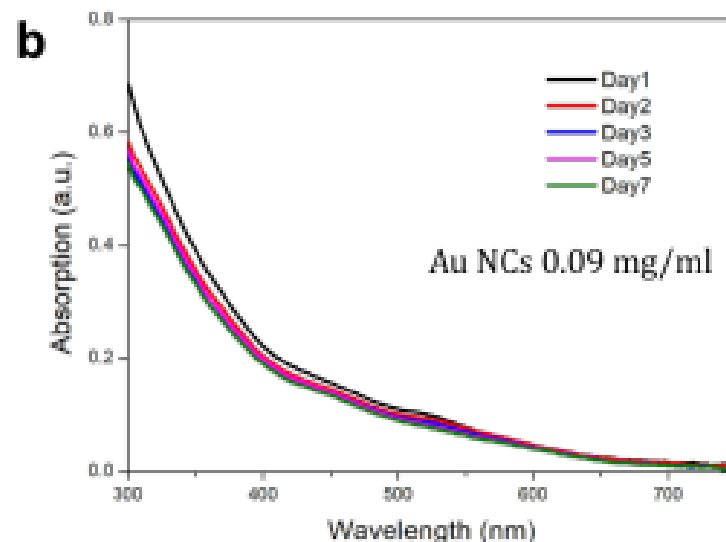
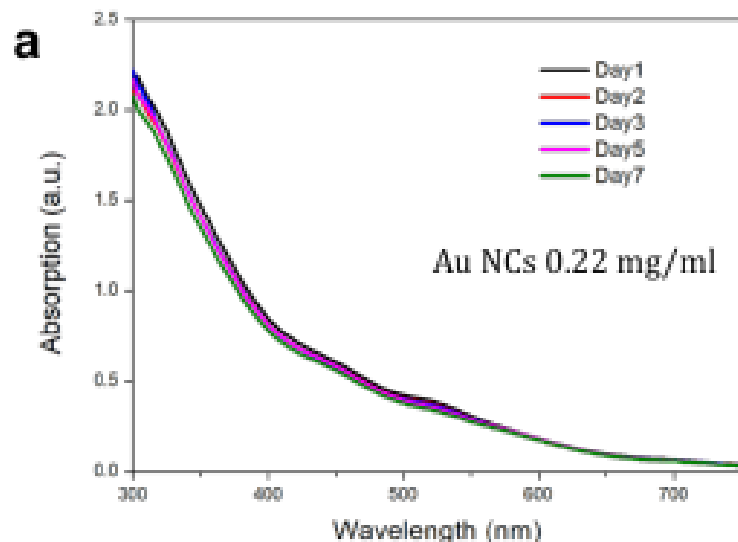
**SIM images of deletional controls.** **a**, the SIM images of bare *M. thermoacetica* without emission under 540 nm excitation. **b**, the SIM image of *M. thermoacetica*-CdS PBS under 408 nm excitation with annular shape emission. The colorcode bar reveals the relative fluorescence intensity, counts ranging from 0 to 3000.



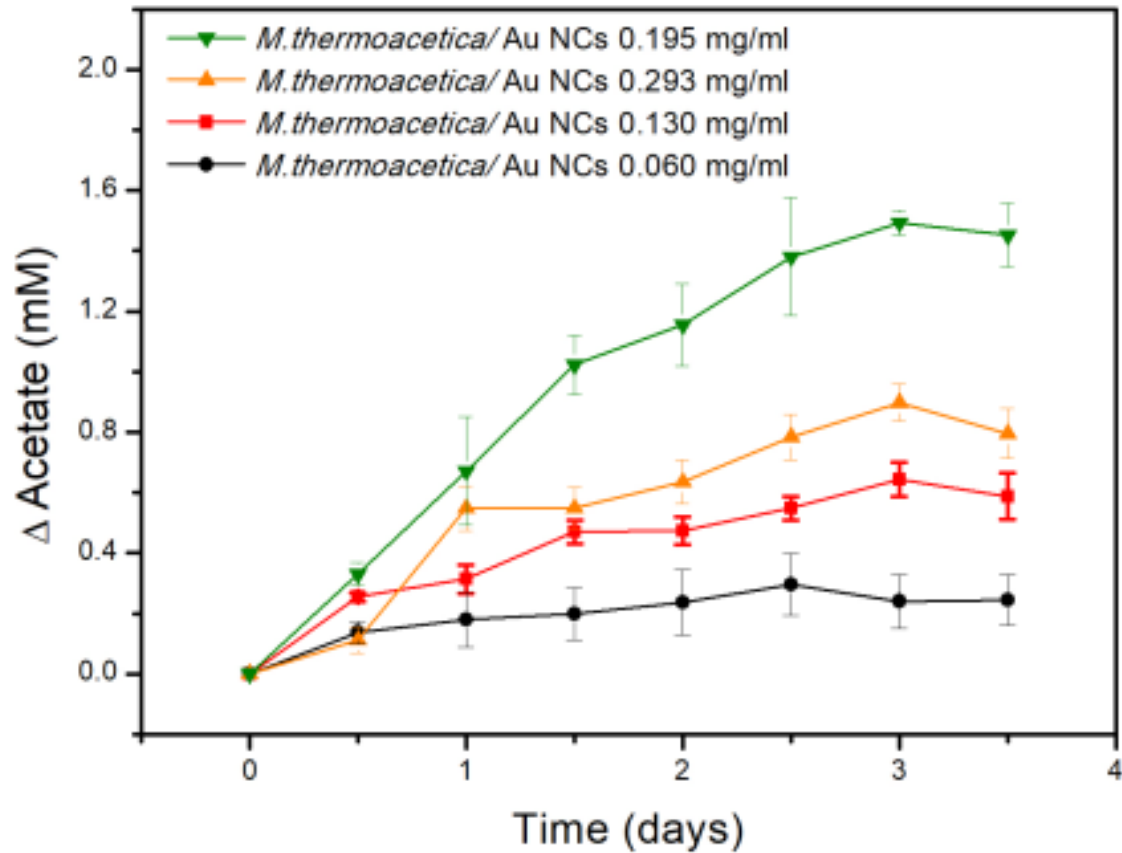
**NMR spectrum.** The NMR spectra of *M. thermoacetica*/Au NCs PBS at different time points with TMSP as the internal standard. The only peak at 1.8 ppm means the acetic acid is the only photosynthesis product in this hybrid system. The timedependent acetic acid production was detected and these spectra are the example for continuous photosynthesis when extra Cys was added after 48 hours reaction.



**Purification of Au<sub>22</sub>(SG)<sub>18</sub> NCs via polyacrylamide gel electrophoresis.** Polyacrylamide gel electrophoresis (PAGE, 30 wt% monomers) was used to separate and collect Au<sub>22</sub>(SG)<sub>18</sub> from Au<sub>15</sub>(SG)<sub>13</sub> and Au<sub>18</sub>(SG)<sub>14</sub>. The pure Au<sub>22</sub>(SG)<sub>18</sub> NCs with unique red emission were used in the *M. thermoacetica*/Au NCs PBSs



**Stability of Au NCs and intracellular Au NCs.** The stability of Au NCs in the medium at different Au NCs concentration 0.22 mg/ml (**a**), 0.09 mg/ml (**b**), and the stability of intracellular Au NCs from day1 to day5 *via* the SIM images with the same excited energy and the same exposure time (**c**). Scale bar for **c** is 1  $\mu\text{m}$ .



**Acetic acid yield.** The photosynthesis efficiencies at different Au concentrations.

## Supplementary Table 4

**Table 4 | Viability assay at different Au NCs concentration.** The viable *M. thermoacetica* in different Au NCs concentrations, the + presents the high viability of *M. thermoacetica* and the – presents the population decay.

Au NCs (mg/ml)	0.060	0.119	0.228	0.293	0.586	0.967	1.898	3.667
Day 0	+	+	+	+	+	+	+	-
Day 1	+	+	+	+	+	+	-	-
Day 2	+	+	+	+	+	-	-	-
Day 3	+	+	+	+	-	-	-	-
Day 4	+	+	+	-	-	-	-	-